Journal of Neurology (2020) 267:2888–2896
https://doi.org/10.1007/s00415-020-09923-z

ORIGINAL COMMUNICATION

BOLD signal within and around white matter lesions distinguishes multiple sclerosis and non-specific white matter disease: a three-dimensional approach

Dinesh K. Sivakolundu[1,6] · Kathryn L. West[1] · Mark D. Zuppichini[1] · Andrew Wilson[3] · Tatum M. Moog[2] · Aiden P. Blinn[2] · Braeden D. Newton[5] · Yeqi Wang[3] · Thomas Stanley[3] · Xiaohu Guo[3] · Bart Rypma[1,4] · Darin T. Okuda[2]

Received: 5 February 2020 / Revised: 12 May 2020 / Accepted: 14 May 2020 / Published online: 28 May 2020

Abstract

Multiple sclerosis (MS) diagnostic criteria are based upon clinical presentation and presence of white matter hyperintensities on two-dimensional magnetic resonance imaging (MRI) views. Such criteria, however, are prone to false-positive interpretations due to the presence of similar MRI findings in non-specific white matter disease (NSWMD) states such as migraine and microvascular disease. The coexistence of age-related changes has also been recognized in MS patients, and this comorbidity further poses a diagnostic challenge. In this study, we investigated the physiologic profiles within and around MS and NSWMD lesions and their ability to distinguish the two disease states. MS and NSWMD lesions were identified using three-dimensional (3D) T_2-FLAIR images and segmented using geodesic active contouring. A dual-echo functional MRI sequence permitted near-simultaneous measurement of blood-oxygen-level-dependent signal (BOLD) and cerebral blood flow (CBF). BOLD and CBF were calculated within lesions and in 3D concentric layers surrounding each lesion. BOLD slope, an indicator of lesion metabolic capacity, was calculated as the change in BOLD from a lesion through its surrounding perimeters. We observed sequential BOLD signal reductions from the lesion towards the perimeters for MS, while no such decreases were observed for NSWMD lesions. BOLD slope was significantly lower in MS compared to NSWM lesions, suggesting decreased metabolic activity in MS lesions. Furthermore, BOLD signal within and around lesions significantly distinguished MS and NSWMD lesions. These results suggest that this technique shows promise for clinical utility in distinguishing NSWMD or MS disease states and identifying NSWMD lesions occurring in MS patients.

Keywords BOLD signal · Non-specific white matter disease · Multiple sclerosis · fMRI

✉ Darin T. Okuda
darin.okuda@UTSouthwestern.edu

1 School of Behavioral and Brain Sciences, University of Texas at Dallas, Dallas, TX, USA

2 Neuroinnovation Program, Multiple Sclerosis & Neuroimmunology Imaging Program, Department of Neurology & Neurotherapeutics, UT Southwestern Medical Center, Dallas, TX, USA

3 Department of Computer Science, University of Texas at Dallas, Dallas, TX, USA

4 Department of Psychiatry, UT Southwestern Medical Center, Dallas, TX, USA

5 Cumming School of Medicine, University of Calgary, Calgary, AB, Canada

6 Department of Biological Sciences, University of Texas at Dallas, Dallas, TX, USA

Introduction

The spatial dissemination criteria for multiple sclerosis (MS) require the presence of white matter lesions seen on magnetic resonance images (MRI) with appropriate size, morphology, location, or temporal characteristics [1]. Such criteria, however, are limited by false-positive determinations due to the presence of similar MRI findings in non-specific white matter disease (NSWMD) states such as migraine, and small vessel diseases [2–6]. Because the criteria were developed to confirm the diagnosis of MS with a classic, clinical presentation [7] or predict the development of MS in a patient with clinically isolated syndrome [8], use of such criteria outside the realm of patients with classic MS clinical presentation leads to a considerable number of NSWMD patients being misclassified [9, 10]. This false fulfillment of

criteria results in patient misdiagnosis, inappropriate treatment, and unnecessary economic burden [10, 11].

Conventional structural MRI studies are highly sensitivity to white matter hyperintensities, but lack specificity regarding disease origin [11, 12]. The coexistence of age-related vascular changes (i.e., NSWMD changes) has been recognized in MS patients, and these comorbidities pose a further diagnostic challenge [13, 14]. Previous research employing more recent MRI techniques (e.g., FLAIR*, magnetization transfer ratio) has attempted to distinguish NSWMD and MS disease states [15, 16]. For instance, FLAIR* can detect the presence of a vein at the center of a white matter lesions (i.e., central vein sign), and such central veins are seen in ~ 80% of MS lesions and in a small proportion of NSWMD lesions [17, 18]. Therefore, the central vein sign with a cut-off of 45% is proficient in distinguishing the two disease states [19]. However, less is known about the distinguishing capacity of these techniques when NSWMD changes coexist with MS [19].

Dual-echo functional MRI (fMRI) provides a means to characterize the etiology of white matter lesions by permitting the assessment of blood oxygenation (i.e., blood-oxygen-level-dependent signal;BOLD) and cerebral blood flow (CBF) within and around lesions [20]. In fMRI, T_2^*-weighted images are highly susceptible to magnetic field inhomogeneities such as hemosiderin and blood oxygenation [21, 22]. Because oxyhemoglobin is weakly diamagnetic and deoxyhemoglobin is strongly paramagnetic, the regional T_2^* decreases as the fraction of deoxyhemoglobin increases. Thus, brain areas with more oxyhemoglobin will have increased BOLD signal (i.e., will appear brighter) than those containing deoxyhemoglobin [22]. In our previous work employing calibrated fMRI in MS patients, we observed that the BOLD signal within and around MS lesions was indicative of the metabolic capacity of the lesion [20]. Thus, using fMRI to metabolically characterize lesions might be informative regarding the source of the insult (i.e., multiple sclerosis, NSWMD).

In this study, we sought to understand whether assessing BOLD and CBF within and around lesions would distinguish MS and NSWMD lesions, irrespective of disease states. Our results indicated that BOLD signal significantly decreases from lesions towards perimeters in MS but not in NSWMD lesions. Thus, MS lesions had a negative BOLD slope compared to NSWMD lesions. Together, assessing BOLD signal within and around MS lesions permitted us to distinguish MS and NSWMD lesion types. Our study shows promise for distinguishing NSWMD and MS disease states, even in situations where NSWMD lesions coexists within MS.

Methods

Research participants

The study group was comprised of MS and non-specific white matter disease (NSWMD) patients recruited from the Clinical Center for Multiple Sclerosis at the University of Texas Southwestern (UTSW) Medical Center and MS patients from local MS support groups. This study group was scanned as part of a larger data collection protocol. MS inclusion criteria were (i) male or female patients between the ages of 18 and 65 with (ii) a diagnosis of a relapsing–remitting MS based on 2010 McDonald criteria [23] confirmed by a specialist in MS (D.T.O) having (iii) an Expanded Disability Status Scale (EDSS) score of 0.0–7.5 and (iv) without any history of migraine or significant vascular risk factors. The inclusion criteria for NSWMD patients were as follows: (i) male or female patients between the ages of 18 and 65, (ii) a history of migraine headaches or small vessel disease risk factors, (iii) focal bilateral supratentorial white matter abnormalities on MRI that are atypical for in situ demyelination (confirmed by a board-certified neuroradiologist) and (iii) the exclusion of a diagnosis of MS by a specialist (D.T.O) based on clinical impressions, radiological features, and the results from other paraclinical studies.

All patients were also required to be (iv) clinically stable (> 90 days) on disease-modifying therapy and (v) treatments for comorbid psychiatric illness (i.e., depression, generalized anxiety disorder), (vi) at least 30 days past their most recent clinical exacerbation and exposure to their last glucocorticosteroid treatment. Exclusion criteria included (i) left-handed patients, (ii) pregnant or nursing women, (iii) history of smoking or cardiopulmonary illness, and (iv) contraindications to MRI. These comprehensive exclusion criteria were designed to eliminate any potential confounds for the larger study aims. As such, we did not anticipate left-handed patients, and those patients with a history of smoking or cardiopulmonary illness, to influence the hemodynamic changes within and around MS or NSWM lesion.

MRI data acquisition

The study was approved by the University of Texas Southwestern (UTSW) Medical Center Institutional Review Board. Written informed consent was obtained from all patients prior to study participation. MRI scans were performed on a Philips 3T MRI scanner equipped with a 32-channel phased array head coil at the UTSW Advanced Imaging Research Center. Participants first underwent a

resting dual-echo fMRI scan wherein they focused their attention on a central fixation cross for the duration of the scan. Following the rest scan, high-resolution T_2-weighted fluid attenuated inversion recovery (T_2-FLAIR), and T_1-weighted magnetization-prepared rapid acquisition gradient-echo (MPRAGE) data were acquired.

Dual-echo fMRI sequence is a time-efficient technique that permits near-simultaneous acquisition of BOLD and CBF data [20, 24–29]. This sequence consists of pseudo-continuous arterial spin labeling (Echo 1, to obtain CBF) and T_2^*- weighted echo-planar acquisition (Echo 2, to obtain BOLD) in an interleaved fashion. Data were acquired with the following scan parameters: TR = 4006 ms, TE_1 = 13 ms, post-label delay = 1450 ms, labeling duration = 1400 ms, labeling RF flip angle = 18°, labeling gap = 63.5 mm, TE_2 = 30 ms, flip angle = 90°, slice gap = 0 mm, FOV = 220 mm × 220 mm × 132 mm, matrix size = 64 × 64, resolution = 3.44 × 3.44 × 6 mm, number of slices = 22.

T_2-FLAIR images were used to identify and segment MS and NSWMD lesions. Data were acquired with the following scan parameters: TR = 4800 ms TE = 344 ms, inversion time (TI) = 1600 ms, slice gap = 0, FOV = 250 mm × 250 mm × 179 mm, matrix size = 228 × 227 × 163, resolution = 1.1mm^3 isotropic, sagittal slice orientation.

MPRAGE images were acquired with the following parameters: repetition time (TR) = 8.1 ms, echo time (TE) = 3.7 ms, resolution = 1mm^3 isotropic, flip angle = 12°, field of view (FOV) = 256 mm × 204 mm × 160 mm, matrix size = 256 × 204 × 160, sagittal slice orientation.

Three-dimensional lesion reconstruction using high-resolution T_2-FLAIR

Lesion segmentation was performed using in-house software allowing for direct extraction of each lesion in 3D space (Fig. 4). White matter lesions from MS and NSWMD patients were first manually identified by an MS specialist (D.T.O.) from simultaneously viewed T_1-weighted and T_2-weighted FLAIR images. The lesion selection criteria were (1) supratentorial lesion location, (2) lesion volume greater than 3mm^3, (3) focal and non-confluent lesions. Selected lesions were segmented from T_2-FLAIR images via geodesic active contour methodology as described by Casseles et al. 1997 [30]. This method allowed us to isolate lesions directly in 3D space. Binary lesion masks were then created from the segmented lesions to study physiologic measures within and around MS and NSWMD lesions.

Cerebral physiology in and around MS lesions

Regions of interest (ROIs)

Cerebral physiology was studied in the lesion and regions around the lesion. Regions around the lesion were defined as 3-mm concentric layers (Fig. 4a, b). The first concentric layer immediately adjacent to the surface of the lesion constituted perimeter 1. The second layer surrounding the surface of the lesion constituted perimeter 2. Regions in the perimeters 1 or 2 that fell within ventricles and extracranium were removed.

Dual-echo fMRI processing

Echo 1 (CBF) and Echo 2 (BOLD) data obtained during dual-echo fMRI were pre-processed using Analysis of Functional Neuroimages (AFNI) software [31]. Data were despiked and realigned to the first functional BOLD volume for each individual using a heptic polynomial interpolation method to correct for motion. CBF was estimated from Echo 1 images (control and label) using surround subtraction [32]. Echo 2 data were neighbor averaged to mitigate the labelling effects from pCASL [32]. Echo 2 data were registered to each participant's anatomical data. The transformation matrix from this registration was then applied to Echo 1 data. Data were then visually inspected and corrected for alignment errors. Echoes 1 and 2 images were then spatially smoothed (8 mm) and high-pass filtered (0.0156 Hz).

Echo 1 data (CBF) were then converted to physiologic units in ml/100 g/min using Buxton's General Kinetic Model for Perfusion Quantification [33, 34]. A cerebrospinal fluid (CSF) ROI was obtained in native space based on a surface-based atlas using FreeSurfer following cortical reconstruction [35]. The CSF mask was used as a reference to calculate equilibrium magnetization of arterial blood (M_0) from Echo 1 control images using the FSL asl_calib program. Estimated values of CBF were masked within range [0–200] ml/100 g/min to exclude implausible physiologic values [36]. CBF and BOLD images were then averaged across time to reduce variability and maximize statistical power resulting in one CBF and BOLD image per participant. Lesion, perimeter 1, and perimeter 2 masks were applied to average baseline CBF maps to obtain CBF in and around MS lesions. Average BOLD signal in the lesion, perimeter 1, and perimeter 2 were obtained as the BOLD signal in these respective regions of interest normalized to the BOLD signal in CSF.

BOLD slope calculation

BOLD slope is the rate of BOLD signal change from each focal MS lesion to perimeters 1 and 2 and was calculated from the best linear fit (see [20]).

Conventional lesion measures (lesion burden, lesion location, and lesion type)

Whole brain lesion burden including focal and confluent lesions was calculated using the lesion prediction algorithm implemented in the LST toolbox version 2.0.15 for SPM. Anatomical lesion location and lesion type were manually defined by an MS specialist (D.T.O).

Statistical analyses

All analyses were performed in R (version 3.4.3) and SPSS (version 24.0). Two-way mixed ANOVA models were performed to test the effects of between- or within-subject factors on physiologic variables, BOLD or CBF. The between-subjects factors were groups (MS or NSWMD), and the within-subjects factors were regions (i.e., lesion and perimeters 1–2). For all models, there were no outliers, as assessed by boxplot. The data were normally distributed, as assessed by Shapiro–Wilk's test of normality. Mauchly's test of sphericity indicated that the assumption of sphericity was violated for the two-way interaction and thus, Greenhouse–Geisser correction was applied. Post-hoc tests were performed using one-way ANOVA and they were Bonferroni-corrected for multiple comparisons. A bionomial logistic regression model was performed to determine if BOLD signal within and around lesions could distinguish MS and NSWMD lesions. The linearity assumption of this regression model was tested using the Box–Tidwell procedure [37]. All continuous variables were linearly related to the logit of the dependent variable.

Results

Lesions

A total of 143 MS lesions were studied from 23 relapsing–remitting MS patients (female = 17 [74%]; median age = 50.1 years [range = 29.6–61.4]; median disease duration = 11.3 years [range = 1.2–30.8]) and 105 NSWMD lesions from 13 NSWMD patients (female = 13 [100%]; median age = 53.9 years [range = 37.8–64.4]). Table 1 summarizes the baseline demographic and clinical data from the study cohort.

BOLD signal within and around MS lesions was altered compared to NSWMD lesions

We sought to assess the changes in blood oxygenation within and around lesions by testing for changes in BOLD signal sequentially moving from lesions to their perimeters between MS and NSWMD lesions.

We tested the hypothesis of group differences in BOLD signal changes from lesions to their perimeters using a 3 (Region) × 2 (Group) mixed ANOVA. MS lesions demonstrated a significant reduction in BOLD signal from the lesion to their surrounding perimeters, $F(1.110, 157.619) = 28.982$, $p < 0.0005$, partial $\eta^2 = 0.170$, (see Fig. 1). No such changes in BOLD signal from lesions to their perimeters were observed in NSWMD lesions, $F(1.085, 112.846) = 0.796$, $p = 0.3836$, partial $\eta^2 = 0.008$. There was a significant Group × Region interaction in BOLD signal, $F(1.105, 271.869) = 10.578$, $p = 0.0009$, partial $\eta^2 = 0.041$. There were no group differences in the acquired BOLD signal when comparing measures within

Table 1 Baseline demographic and clinical data from the study cohort

Characteristics	Multiple sclerosis patients (number of patients = 23)	Non-specific white matter disease patients (number of patients = 13)
Age (years) Median (range)	50.1 (29.6–61.4)	53.9 (37.8–64.4)
Female sex Number (%)	17 (74%)	13 (100%)
Disease duration (years) Median (range)	11.3 (1.2–30.8)	–
Patients on disease-modifying therapy Number (%)	16 (69.6%)	–
Age at diagnosis (years) Median (range)	38 (26–54)	–
Time since last acute exacerbation (years) Median (range)	2.8 (0.4–13.3)	–
Expanded Disability Status Scale score Median (range)	2.5 (1–7.5)	–
Total lesion volume (ml) Median (range)	3.035 (0.12–26.32)	1.3428 (0.27–13.0863)

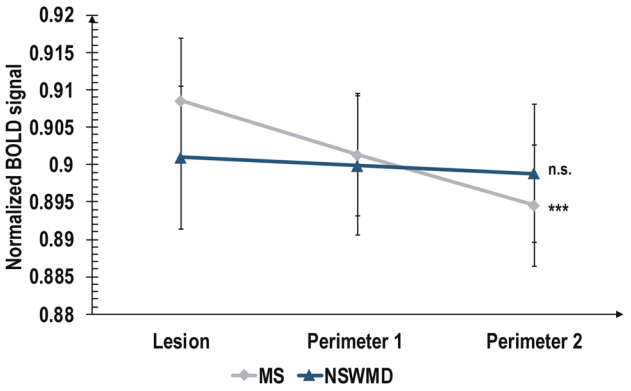

Fig. 1 Mean blood-oxygen-level-dependent (BOLD) signal in lesions and their perimeters for multiple sclerosis (MS; grey) and non-specific white matter lesions (NSWMD; blue). ***$p < 0.0005$, n.s. is $p > 0.05$

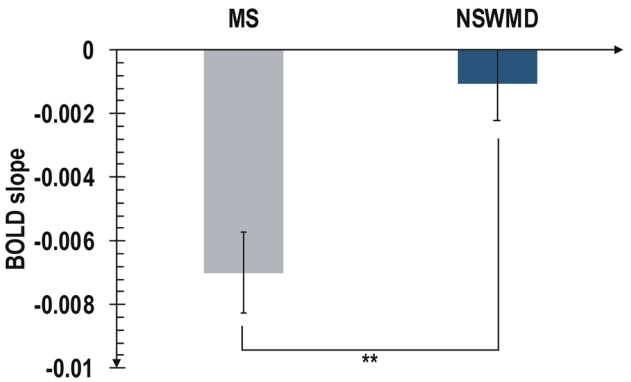

Fig. 2 Bar graph representing mean BOLD slope for MS and NSWMD lesions. **$p < 0.005$

lesion tissue ($p > 0.05$), perimeter 1 ($p > 0.05$), and perimeter 2 ($p > 0.05$).

BOLD slope was significantly lower in NSWMD lesions compared to MS lesions

Our previous work has shown that BOLD slope is an indicator of metabolic capacity within and around MS lesions [20]. We assessed metabolic differences between MS and NSWMD lesions by testing for group differences in BOLD slope using an independent-sample *t* test. BOLD slope was significantly lower in MS lesions ($M_{MS} = -0.0070$, $SD_{MS} = 0.0151$) compared to NSWMD lesions ($M_{NSWMD} = -0.0011$, $SD_{NSWMD} = 0.0118$, $t(245.026) = -3.471$, $p = 0.0006$, see Fig. 2).

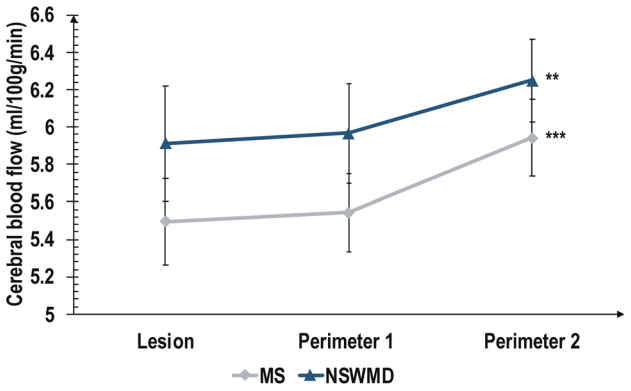

Fig. 3 Mean cerebral blood flow in lesions and their perimeters for multiple sclerosis (grey) and non-specific white matter lesions (blue). ***$p < 0.0005$, **$p < 0.005$

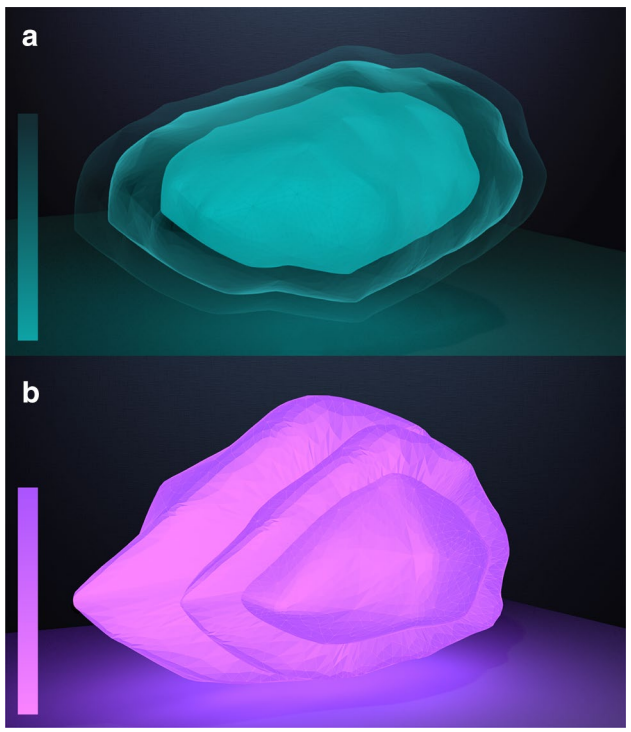

Fig. 4 Three-dimensional illustration of a multiple sclerosis lesion and its perimeters (**a**), and a non-specific white matter lesion and its perimeters (**b**). The color scale represents the change in the blood-oxygen-level-dependent signal. Darker portions of the color scale represent a higher BOLD signal and lighter portions represent lower BOLD signal values. Note the gradual reduction in BOLD signal from the lesion to its perimeters for the MS lesion (**a**) with no such reductions observed for the NSWMD lesion (**b**)

CBF was not altered within and around MS lesions and NSWMD lesions

We sought to assess the changes in CBF within and around lesions by testing for changes in CBF sequentially moving

from lesions to their perimeters between MS and NSWMD lesions.

We tested the hypothesis of group differences in CBF changes from lesions to their perimeters using a 3 (Region) × 2 (Group) mixed ANOVA. We observed that CBF sequentially increased from lesions to perimeters in MS and NSWMD (see Fig. 3). CBF significantly increased moving from lesions to their perimeters for both MS ($F(1.117, 158.595) = 15.487$, $p < 0.0005$, partial $\eta^2 = 0.098$) and NSWMD lesions ($F(1.050, 109.233) = 5.182$, $p = 0.0063$, partial $\eta^2 = 0.047$). There was no significant Group × Region interaction in CBF, $F(1.085, 266.994) = 0.428$, $p = 0.5299$, partial $\eta^2 = 0.002$. Differences in CBF within lesion tissue ($p > 0.05$) and in the surrounding perimeters ($p > 0.05$) when comparing MS and NSWMD lesions were also not observed.

BOLD signal within and around lesions significantly distinguished NSWMD from MS lesions

We sought to assess whether blood oxygenation within and around MS lesions could inform on the origin of the observed white matter lesions (i.e., MS, NSWMD). To test this hypothesis, binomial logistic regression was performed with Groups as a dependent variable and BOLD slope as an independent variable. The logistic regression model was statistically significant, $\chi^2(1) = 11.598$, $p = 0.0007$. The specificity of the model in identifying NSWMD lesion was 76.9%. The sensitivity was 31.4%. With increase in BOLD slope, there was an increased likelihood of a lesion being due to NSWMD (β coefficient = 34.068, standard error = 10.671, $\text{Exp}(\beta) = 6.242\text{E}+14$, $\text{Wald}(1) = 10.192$, $p = 0.0014$).

Discussion

In the present study, we sought to distinguish MS and NSWMD disease by investigating the physiologic profiles within and around lesions. Traditionally, clinicians have utilized MRI to identify white matter hyperintensities using two-dimensional anatomical planes of view (i.e., axial, sagittal, and coronal) to define these two diseases states. We quantified BOLD signal and CBF using dual-echo fMRI through a novel technique assessing the physiologic data in three-dimensional space within the lesion and its surrounding concentric perimeters exact to the lesion's external shape. While MS lesions exhibited BOLD signal decreases extending from lesions towards perimeters, NSWMD lesions exhibited no such decreases (Figs. 1, 4). Furthermore, BOLD signal changes from perimeters to lesions significantly distinguished NSWMD lesions from MS lesions. The ability of this technique to distinguish the two disease states at the level of individual lesions suggests its prospects for clinical utility in distinguishing NSWMD and MS diseases separately and when NSWMD changes coexist with MS [10, 11].

The BOLD signal characteristics observed in MS lesions might be related to underlying physiologic changes given the sensitivity to the presence of paramagnetic factors that induce magnetic field inhomogeneities such as hemosiderin (i.e., iron deposits) and deoxyhemoglobin [22]. As veins are rich in deoxyhemoglobin, and the regional T_2^* relaxation time decreases as the fraction of deoxyhemoglobin increases, BOLD reflects venous oxygen content. Because the venous oxygen content depends on factors such as arterial CBF, cellular oxygen extraction from the capillaries, and cerebral metabolic rate of oxygen, the observed group differences in BOLD signal in lesions, and their perimeters might reflect neurometabolic differences between MS and NSWMD.

The metabolic impact of lesions on adjacent tissue might be an important contributor to the physiologic differences observed between MS and NSWMD lesions. On one hand, tissue within MS lesions is subjected to a virtual hypoxic state caused by an imbalance between energy demand and supply [38]. This hypoxic state might be due to impaired mitochondrial energy production [39], reductions in CBF itself [40], or a combination of these factors. We observed that MS lesions have increased venous blood oxygenation compared to their surroundings without changes in arterial CBF. On the other hand, tissue within NSWMD lesions undergoes only a minimal imbalance between energy demand and supply. This minimal imbalance might be due to angiogenesis, and brain plasticity resulting from a previous micro-thrombotic event that manifests as non-specific white matter hyperintensity [41, 42]. Thus, we observed no alterations in surrounding venous oxygenation or arterial blood flow in NSWMD lesions. Furthermore, we observed reductions in BOLD slope from the lesion outward, an indicator of metabolic capacity of lesions [20] in MS lesions compared to NSWMD lesions. Together, these results implicate different metabolic and physiologic signatures of MS and NSWMD lesions and their surrounding tissue providing the potential to differentiate the two disease states.

We observed BOLD differences with no CBF differences within and around MS and NSWMD lesions. The dual-echo measurements (i.e., BOLD and CBF) reflect the integrity of different vessel types. Cerebral blood flow reflects the integrity of the arterial system. Because the BOLD signal relies on the ratio of diamagnetic oxygenated to paramagnetic deoxygenated hemoglobin and arteries are nearly 100% oxygen saturated, BOLD contrast mainly emerges from the venous blood oxygenation, and thus BOLD signal reflects the integrity of the venous system [29, 43]. Thus, we hypothesize that alterations in different vessel types within and around lesions might lead to our observation of BOLD signal changes in these regions with CBF changes.

Previous literature investigating CBF changes within lesions suggested marked heterogeneity between lesion types [44, 45]. For instance, a study utilizing dynamic susceptibility contrast MR imaging found that CBF was lower in MS lesions compared to normal white matter in healthy controls [44]. However, contrast-enhancing MS lesions demonstrated increased CBF compared to normal white matter in healthy controls. This result is consistent with work from our lab demonstrating that CBF was lower in metabolically inactive MS lesions compared to metabolically active MS lesions [20]. Future studies are, however, required to investigate how CBF changes between enhancing, non-enhancing MS lesions, and NSWMD lesions.

Our technique of assessing BOLD signal within and around lesions shows promise for distinguishing MS and NSWMD lesions. Traditionally, clinicians have relied upon a combination of T_1- and T_2-weighted anatomical images to observe lesion features such as lesion location and shape that are suggestive of either MS or NSWMD [12, 46]. For instance, NSWMD lesions spare U-fibers, affect the central pons, and are associated with lacunae and microbleeds [47]. Although such traditional techniques have increased sensitivity in identifying these NSWMD lesions, they lack specificity for accurately distinguishing NSWMD lesion from MS lesions [10]. Newer techniques, such as the T_2^*- or FLAIR*-weighted images, that identify the presence of a central vein within the lesions or magnetic resonance spectroscopy that identifies specific metabolites in the brain (e.g., choline, lactate, lipid, and N-acetyl aspartate), have improved specificity in distinguishing the two disease states compared to the traditional methods [18, 48]. Studies investigating the central vein within lesions have established the presence of 45% of lesions with central veins in a patient to be highly suggestive of MS. However, this technique might be limited in older MS patients and in MS patients with coexisting vascular abnormalities [19]. The technique of assessing BOLD signal within and around lesions, and BOLD signal change from lesions towards the perimeters employed in this study, may be able to differentiate NSWMD lesions from MS lesions at the level of individual lesions and thus, can be employed even in older MS lesions and MS patients with coexisting vascular abnormalities or NSWMD changes.

This study proposes a novel technique to distinguish MS and NSWMD lesions. There are, however, certain limitations associated with the study. We considered lesions classified as MS and NSWMD by an MS expert as the gold standard based on historical, clinical, and radiological data. This method was employed due to the lack of pre-mortem histopathological specimens from patients. In addition, this technique is currently limited in its ability to study the surrounding tissue of lesions that have coalesced. Thus, validating this technique with lesion histopathology in animal models, and in a larger sample study will be necessary. This study is also limited by low resolution of the BOLD maps reducing the ability to study finer details within lesions and their perimeters, and potential partial volume effects due to the low resolution. Further studies involving the metabolic signature of lesions and perimeter 1 employing higher-resolution BOLD imaging techniques are needed to improve our understanding of the value of this approach in differentiating between these the two disease states. Future studies will also be necessary to investigate the effects of susceptibility rings or central vein in MS lesions on hemodynamic changes.

In conclusion, alternative approaches beyond the evaluation of structural characteristics are needed to improve the specificity of lesion origin. We demonstrated that the physiological characteristics within lesions and in surrounding tissue may improve our disease characterization. In the future, these data may have utility at the individual patient or lesion level. Overall, this technique shows promise for clinical utility to distinguish the two disease states and effectively adds to other methods that aim to improve the specificity in identifying the etiology of central nervous system lesions to optimize the quality of medical management provided to the patients we serve.

Acknowledgements We thank all the patients and volunteers who participated in this research efforts. We thank our lab research interns and coordinators for their help in recruiting patients and volunteering for the study. Special thanks to Jeffery Spence, and Hanzhang Lu for their scientific input regarding the study. Funding: This work was supported by a National Multiple Sclerosis Society Research Grant (RG-1507-04951) to BR and DO.

Compliance with ethical standards

Conflicts of interest KW, MZ, AW, XG, TM, AB, YW, TS, and BR report no disclosures. DO received advisory and consulting fees from Celgene, EMD Serono, Genentech, Genzyme, and Novartis and research support from Biogen. DS, BN, and DO have a patent pending related to the submitted work.

Ethics approval This study was approved by the University of Texas Southwestern Medical Center Institution Review Board. Written informed consent was obtained from all participants prior to study participation.

References

1. Thompson AJ, Banwell BL, Barkhof F et al (2018) Diagnosis of multiple sclerosis: 2017 revisions of the McDonald criteria. Lancet Neurol 17:162–173. https://doi.org/10.1016/S1474-4422(17)30470-2
2. Liu S, Kullnat J, Bourdette D et al (2013) Prevalence of brain magnetic resonance imaging meeting Barkhof and McDonald criteria for dissemination in space among headache patients. Mult Scler J 19(8):1101–1105. https://doi.org/10.1177/1352458512471874

3. Seneviratne U, Chong W, Billimoria PH (2013) Brain white matter hyperintensities in migraine: clinical and radiological correlates. Clin Neurol Neurosurg. https://doi.org/10.1016/j.clineuro.2012.10.033
4. Absinta M, Rocca MA, Colombo B et al (2012) Patients with migraine do not have MRI-visible cortical lesions. J Neurol. https://doi.org/10.1007/s00415-012-6571-x
5. Akman-Demir G, Mutlu M, Kiyat-Atamer A et al (2015) Behçet's disease patients with multiple sclerosis-like features: discriminative value of Barkhof criteria. Clin Exp Rheumatol 33:S80–S84
6. Kim SS, Richman DP, Johnson WO et al (2014) Limited utility of current MRI criteria for distinguishing multiple sclerosis from common mimickers: primary and secondary CNS vasculitis, lupus and Sjogren's syndrome. Mult Scler. https://doi.org/10.1177/1352458513491329
7. Thompson AJ, Banwell BL, Barkhof F et al (2018) Diagnosis of multiple sclerosis: 2017 revisions of the McDonald criteria THOMPSON, A. J. et al. Diagnosis of multiple sclerosis: 2017 revisions of the McDonald criteria. Lancet Neurol 17(2):162–173. https://doi.org/10.1016/S1474-4422(17)30470-2
8. Barkhof F, Filippi M, Miller DH et al (1997) Comparison of MRI criteria at irst presentation to predict conversion to clinically deinite multiple sclerosis. Brain 120(11):2059–2069. https://doi.org/10.1093/brain/120.11.2059
9. Toledano M, Weinshenker BG, Solomon AJ (2015) A clinical approach to the differential diagnosis of multiple sclerosis. Curr Neurol Neurosci Rep 15(8):57. https://doi.org/10.1007/s11910-015-0576-7
10. Solomon AJ, Weinshenker BG (2013) Misdiagnosis of multiple sclerosis: frequency, causes, effects, and prevention. CurrNeurol Neurosci Rep. https://doi.org/10.1007/s11910-013-0403-y
11. Solomon AJ, Bourdette DN, Cross AH et al (2016) The contemporary spectrum of multiple sclerosis misdiagnosis: a multicenter study. Neurology 87:1393–1399. https://doi.org/10.1212/WNL.0000000000003152
12. Geraldes R, Ciccarelli O, Barkhof F et al (2018) The current role of MRI in differentiating multiple sclerosis from its imaging mimics. Nat Rev Neurol 14:199–213. https://doi.org/10.1038/nrneurol.2018.14
13. Schmidt R, Enzinger C, Ropele S et al (2006) Subcortical vascular cognitive impairment: Similarities and differences with multiple sclerosis. J Neurol Sci. https://doi.org/10.1016/j.jns.2005.06.018
14. Geraldes R, Esiri MM, Deluca GC, Palace J Age-related small vessel disease: a potential contributor to neurodegeneration in multiple sclerosis. https://doi.org/10.1111/bpa.12460
15. Giorgio A, De Stefano N (2016) Advanced structural and functional brain MRI in multiple sclerosis. Semin Neurol. https://doi.org/10.1055/s-0036-1579737
16. Rocca MA, Colombo B, Pratesi A et al (2000) A magnetization transfer imaging study of the brain in patients with migraine. Neurology 54:507–507. https://doi.org/10.1212/WNL.54.2.507
17. Mistry N, Abdel-Fahim R, Samaraweera A et al (2016) Imaging central veins in brain lesions with 3-T T2*-weighted magnetic resonance imaging differentiates multiple sclerosis from microangiopathic brain lesions. Mult Scler. https://doi.org/10.1177/1352458515616700
18. Samaraweera APR, Clarke MA, Whitehead A et al (2017) The central vein sign in multiple sclerosis lesions is present irrespective of the T2* sequence at 3 T. J Neuroimaging 27:114–121. https://doi.org/10.1111/jon.12367
19. Sati P, Oh J, Todd Constable R et al (2016) The central vein sign and its clinical evaluation for the diagnosis of multiple sclerosis: a consensus statement from the North American Imaging in Multiple Sclerosis Cooperative. Nat Rev Neurol. https://doi.org/10.1038/nrneurol.2016.166
20. Sivakolundu DK, Hansen MR, West KL et al (2019) Three-dimensional lesion phenotyping and physiologic characterization inform remyelination ability in multiple sclerosis. J Neuroimaging 00:1–10. https://doi.org/10.1111/jon.12633
21. Ogawa S, Lee TM, Kay AR, Tank DW (1990) Brain magnetic resonance imaging with contrast dependent on blood oxygenation. Proc Natl Acad Sci 87(24):9868–9872. https://doi.org/10.1073/pnas.87.24.9868
22. Kim S-G, Ogawa S (2012) Biophysical and physiological origins of blood oxygenation level-dependent fMRI signals. J Cereb Blood Flow Metab 32:1188–1206. https://doi.org/10.1038/jcbfm.2012.23
23. Polman CH, Reingold SC, Banwell B, et al Diagnostic criteria for multiple sclerosis: 2010 revisions to the McDonald criteria. https://doi.org/10.1002/ana.22366
24. Sivakolundu DK, West KL, Maruthy GB et al (2019) Reduced arterial compliance along the cerebrovascular tree predicts cognitive slowing in multiple sclerosis: evidence for a neurovascular uncoupling hypothesis. Mult Scler J. https://doi.org/10.1177/1352458519866605
25. Sivakolundu DK, West KL, Zuppichini M et al (2020) The neurovascular basis of processing speed diferences in humans: a model-systems approach using multiple sclerosis. NeuroImage. https://doi.org/10.1016/j.neuroimage.2020.116812
26. Altered task-induced cerebral blood flow and oxygen metabolism underlies motor impairment in multiple sclerosis - Kathryn L West, Dinesh K Sivakolundu, Mark D Zuppichini, Monroe P Turner, Jeffrey S Spence, Hanzhang Lu, Darin T Okuda, Bart Rypma. https://journals.sagepub.com/doi/abs/10.1177/0271678X20908356. Accessed 5 May 2020
27. Hutchison JL, Lu H, Rypma B (2013) Neural mechanisms of age-related slowing: the ΔCBF/ΔCMRO2 ratio mediates age-differences in BOLD signal and human performance. Cereb Cortex 23:2337–2346
28. Hoge RD, Atkinson J, Gill B et al (1999) Investigation of BOLD signal dependence on cerebral blood flow and oxygen consumption: the deoxyhemoglobin dilution model. Magn Reson Med 863:849–863
29. Hoge RD, Atkinson J, Gill B et al (1999) Linear coupling between cerebral blood flow and oxygen consumption in activated human cortex. Proc Natl Acad Sci 96:9403–9408
30. Caselles V, Kimmel R, Sapiro G (1997) Geodesic active contours. Kluwer Academic Publishers, Berlin
31. Cox RW (1996) AFNI: software for analysis and visualization of functional magnetic resonance neuroimages. Comput Biomed Res 29:162–173. https://doi.org/10.1006/cbmr.1996.0014
32. Liu TT, Wong EC (2005) A signal processing model for arterial spin labeling functional MRI. NeuroImage 24:207–215. https://doi.org/10.1016/J.NEUROIMAGE.2004.09.047
33. Alsop DC, Detre JA, Golay X et al (2015) Recommended implementation of arterial spin-labeled perfusion MRI for clinical applications: a consensus of the ISMRM perfusion study group and the European consortium for ASL in dementia. Magn Reson Med 73:102–116. https://doi.org/10.1002/mrm.25197
34. Buxton RB, Wong EC, Frank LR (1998) Dynamics of blood flow and oxygenation changes during brain activation: the balloon model. Magn Reson Med 39:855–864. https://doi.org/10.1002/mrm.1910390602
35. Desikan RS, Ségonne F, Fischl B et al (2006) An automated labeling system for subdividing the human cerebral cortex on MRI scans into gyral based regions of interest. NeuroImage 31:968–980. https://doi.org/10.1016/J.NEUROIMAGE.2006.01.021
36. Merola A, Germuska MA, Warnert EA et al (2017) Mapping the pharmacological modulation of brain oxygen metabolism: the effects of caffeine on absolute CMRO2 measured using

dual calibrated fMRI. NeuroImage 155:331–343. https://doi.org/10.1016/J.NEUROIMAGE.2017.03.028
37. Box GEP, Tidwell PW (2012) Transformation of the independent variables. Technometrics 4(4):531–550. https://doi.org/10.1080/00401706.1962.10490038
38. Trapp BD, Stys PK (2009) Virtual hypoxia and chronic necrosis of demyelinated axons in multiple sclerosis. www.thelancet.com/neurology8. https://doi.org/10.1016/S1474-4422(09)70043-2
39. Dutta R, Mcdonough J, Yin X et al (2006) Mitochondrial dysfunction as a cause of axonal degeneration in multiple sclerosis patients. Ann Neurol 59:478–489. https://doi.org/10.1002/ana.20736
40. Belov P, Jakimovski D, Krawiecki J et al (2018) Lower arterial cross-sectional area of carotid and vertebral arteries and higher frequency of secondary neck vessels are associated with multiple sclerosis. AJNR Am J Neuroradiol 39:123–130. https://doi.org/10.3174/ajnr.A5469
41. Porter A, Gladstone JP, Dodick DW (2005) Migraine and white matter hyperintensities. Curr Pain Headache Rep 9(4):289. https://doi.org/10.1007/s11916-005-0039-y
42. Galluzzi S, Lanni C, Pantoni L et al (2008) White matter lesions in the elderly: pathophysiological hypothesis on the efect on brain plasticity and reserve. J Neurol Sci 273(1–2):3–9. https://doi.org/10.1016/j.jns.2008.06.023
43. Abdelkarim D, Zhao Y, Turner MP et al (2019) A neural-vascular complex of age-related changes in the human brain: anatomy, physiology, and implications for neurocognitive aging. Neurosc Biobehav Rev 107:927–944. https://doi.org/10.1016/j.neubiorev.2019.09.005
44. Ge Y, Law M, Johnson G et al (2005) Dynamic susceptibility contrast perfusion MR imaging of multiple sclerosis lesions: characterizing hemodynamic impairment and inflammatory activity. Am J Neuroradiol 26:1539–1547
45. Lucchinetti C, Brück W, Parisi J et al (2000) Heterogeneity of multiple sclerosis lesions: Implications for the pathogenesis of demyelination. Ann Neurol 47:707–717. https://doi.org/10.1002/1531-8249(200006)47:6%3c707:AID-ANA3%3e3.0.CO;2-Q
46. Filippi M, Rocca MA, Ciccarelli O et al (2016) MRI criteria for the diagnosis of multiple sclerosis: MAGNIMS consensus guidelines. Lancet Neurol 15:292–303. https://doi.org/10.1016/S1474-4422(15)00393-2
47. Chen JJ, Carletti F, Young V et al (2016) MRI diferential diagnosis of suspected multiple sclerosis. Clin Radiol 71(9):815–827. https://doi.org/10.1016/j.crad.2016.05.010
48. Filippi M, Rocca MA (2008) Multiple sclerosis and allied white matter diseases. Neurol Sci. https://doi.org/10.1007/s10072-008-1007-1